Maintaining Chaos in High Dimensions

Visarath In,[1] Mark L. Spano,[1] and Mingzhou Ding[2]
[1]*Naval Surface Warfare Center, Code 684, 9500 MacArthur Boulevard, West Bethesda, Maryland 20817*
[2]*Center for Complex Systems and Department of Mathematical Sciences, Florida Atlantic University, Boca Raton, Florida 33431*
(Received 1 August 1997)

In dynamical systems, as a parameter is varied past a critical value, a chaotic attractor may be destroyed by a crisis. This attractor is replaced by a chaotic transient, which eventually leads to a different attractor. We present a method for maintaining chaotic dynamics after the crisis. The model, formulated for arbitrary dimensions, directs the phase space trajectory toward a target region near the periodic saddle orbit that mediates the crisis. It is used to maintain chaos numerically in the Ikeda map and experimentally in a magnetoelastic ribbon. [S0031-9007(97)05100-4]

PACS numbers: 05.45.+b, 75.80.+q

Chaos possesses many desirable properties. It can enhance the mixing of fluids [1]. In biology, the absence of chaos has been implicated in disease [2]. In an industrial application, the thermal pulse combustor operates chaotically when running with a lean fuel/air mixture [3]. But attempts to improve fuel efficiency (by making the mixture even leaner than some critical ratio) can destroy the chaos and cause the combustor to flameout [4].

Techniques to preserve and maintain chaos have recently received considerable attention. Experiments to increase the disorder found in the electrical firings of rat hippocampal neurons used an *ad hoc* method of maintaining chaos (therein called *anticontrol*) to drive the system state off of the chaotic attractor whenever it approached a given periodic saddle point [5]. Later Yang *et al.* [6] proposed a method that used an *analytical* knowledge of the system dynamics to map preiterates of an escape region and to determine a minimal perturbation. It is applied as the system enters one of the preiterate regions to prevent it from eventually entering the escape region. This method was successful in a number of analytical models but has not been experimentally realized due to the difficulty of extracting accurate models for experimental systems. An experimentally effective refinement [7] uses only information derived from experimental data. The shortcoming of this method lies in its semiempirical nature. A different method [8] for maintaining chaos uses feedback control of Lyapunov exponents so that they are all made positive.

None of these make explicit use of the insight that the destruction of chaotic attractors often occurs during *crises*. After a crisis, the system behaves chaotically for an extended period of time until it nears the periodic saddle point that *mediates* the crisis. The system is ejected from the basin of attraction of the former chaotic attractor. Schwartz and Triandaf [9] used local knowledge of the mediating orbit to put the system back into the transient region before the orbit escaped to the other attractor. But their method is restricted to crises where the mediating saddle has one stable and one unstable manifold.

In this paper we develop a systematic method for maintaining chaos that is applicable to high-dimensional systems and can be easily implemented experimentally. It uses a discrete time series generated by a Poincaré section of the original continuous-time phase space. By varying a single system parameter, our method maintains chaos using the dynamics of a mediating saddle having any number of stable or unstable manifolds. We demonstrate it both computationally on an Ikeda map and experimentally in a magnetoelastic ribbon experiment with a mediating saddle containing one unstable direction and two complex stable directions.

Basic concept and mathematical formulation of the method.—For illustration, consider a 2D map. We assume that a period one saddle point mediates the crisis [10]. The dynamics around this saddle is such that one branch of the unstable manifold leads to a different attractor, while the other leads back into the remnant of the chaotic attractor. Immediately after the crisis, a trajectory can bounce around on the chaotic remnant for some time before it escapes to the other attractor via the neighborhood of the mediating saddle [10]. This suggests that, when the orbit comes near the mediating saddle, we use properties of the saddle and small perturbations to steer the orbit to a predetermined target point along the unstable branch leading toward the chaotic remnant. Then, after the control is turned off, the natural dynamics will take the orbit back to the chaotic remnant. Our choice of the target point is the first iterate of the point that is a distance ε away from the period-1 saddle along the unstable manifold. Here ε is the maximum noise amplitude. In this fashion we guard against the trajectory being knocked into the other attractor's basin by noise. Next we implement these considerations mathematically for arbitrary dimensions.

Suppose that the system is described by a Poincaré map, $\mathbf{X}_{n+1} = \mathbf{F}(\mathbf{X}_n, p)$, where $\mathbf{X}_n \in \mathbf{R}^k$ and p is a system parameter chosen for maintaining chaos. p need not be the parameter whose change causes the crisis. Assume that the dynamical equations describing the system are

 0031-9007/98/80(4)/700(4)$15.00

not known, but that a time series $\{x_n\}$ of some scalar observable $x_n = h(\mathbf{X}_n)$ can be measured via a measurement function h. Using delay coordinate embedding [11], we reconstruct the dynamics as $\mathbf{z}_n = (z_n^{(1)}, z_n^{(2)}, \ldots, z_n^{(m)})^T = (x_{n-m+1}, x_{n-m+2}, \ldots, x_n)^T$, where m is the dimension of the reconstructed phase space. For large enough m, $\mathbf{z}_n$ is a global one-to-one representation of $\mathbf{X}_n$ [11]. In addition, since one must change the parameter p according to a control law at every iteration of the map in the vicinity of the mediating saddle, the reconstructed discrete map for $\mathbf{z}_n$ has the form $\mathbf{z}_{n+1} = \mathbf{G}(\mathbf{z}_n, p_{n-m+1}, p_{n-m+2}, \ldots, p_n)$. Here $\mathbf{G}$ necessarily depends on all the parameter variations effective during the time interval $n - m + 1 \le t \le n$ spanned by the delay vector $\mathbf{z}_n$ [12]. For simplicity we derive the control law used to maintain chaos for the case where the mediating saddle is a fixed point.

The saddle point in the delay coordinate space is denoted by $\mathbf{z}^*(p^*) = \mathbf{G}[\mathbf{z}^*(p^*), p^*, p^*, \ldots, p^*]$. Here p^* is the nominal value of the control parameter. Paralleling Ref. [13], we introduce the following $m \times m$ Jacobian matrix, $\mathbf{A}_n = \mathbf{D}_{\mathbf{z}_n}\mathbf{G}(\mathbf{z}_n, p_{n-m+1}, p_{n-m+2}, \ldots, p_n)$, to describe the linearized dynamics near the saddle point, and a set of m-dimensional column vectors to describe the effect of the control parameter variations on the dynamics, $\mathbf{B}_n^{(1)} = \mathbf{D}_{p_{n-i+1}}\mathbf{G}(\mathbf{z}_n, p_{n-m+1}, p_{n-m+2}, \ldots, p_n)$, $i = 1, 2, \ldots, m$. Evaluating all the partial derivatives at the saddle point, $\mathbf{z}_n = \mathbf{z}^*(p^*)$ and setting $p_{n-m+1} = p_{n-m+2} = \cdots = p_n = p^*$, we obtain the linearization:

$$\delta\mathbf{z}_{n+1} = \mathbf{A}\cdot\delta\mathbf{z}_n + \mathbf{B}^{(m)}\delta p_{n-m+1} + \mathbf{B}^{(m-1)}\delta p_{n-m+2} + \cdots + \mathbf{B}^{(1)}\delta p_n, \quad (1)$$

where $\delta\mathbf{z}_n \equiv \mathbf{z}_n - \mathbf{z}^*(p^*)$, $\delta p_n \equiv p_n - p^*$ and we drop the reference to n for $\mathbf{A}$ and the $\mathbf{B}$'s. Because of the nature of the time series and delay coordinates used, $\mathbf{A}$ and the $\mathbf{B}$'s are sparse:

$$\mathbf{A} = \begin{pmatrix} 0 & 1 & 0 & \cdots & 0 \\ 0 & 0 & 1 & \cdots & 0 \\ \vdots & \vdots & \vdots & \vdots & \vdots \\ 0 & 0 & 0 & \cdots & 1 \\ a^{(m)} & a^{(m-1)} & a^{(m-2)} & \cdots & a^{(1)} \end{pmatrix}_{m\times m} \quad \text{and} \quad \mathbf{B}^{(i)} = \begin{pmatrix} 0 \\ 0 \\ \vdots \\ 0 \\ b^{(i)} \end{pmatrix}_{m\times 1}, \qquad i = 1, 2, \ldots, m. \quad (2)$$

Without loss of generality, assume that $\mathbf{A}$ has u unstable directions and s stable directions; i.e., $u + s = m$ with eigenvalues λ_i satisfying $|\lambda_1| > |\lambda_2| > \cdots > |\lambda_u| > 1 > |\lambda_{u+1}| > |\lambda_{u+2}| > \cdots > |\lambda_m|$. Let $\mathbf{e}_i$ be the corresponding normalized eigenvectors. It is undesirable to derive control laws directly based on Eq. (1) [12]. Following So and Ott [14] consider an expanded $(2m-1)$-dimensional phase space, $\mathbf{Y}_n = (\mathbf{z}_n^T, p_{n-m+1}, p_{n-m+2}, \ldots, p_{n1})^T$, to accommodate both the dynamical measurements and the parameter changes. The linearized dynamics of the saddle point in the expanded phase space is $\mathbf{Y}_{n+1} - \mathbf{Y}^* = \tilde{\mathbf{A}}(\mathbf{Y}_n - \mathbf{Y}^*) + \tilde{\mathbf{B}}(p_n - p^*)$, where

$$\tilde{\mathbf{A}} = \begin{pmatrix} \mathbf{A} & \mathbf{B}^{(m)} & \mathbf{B}^{(m-1)} & \cdots & \mathbf{B}^{(2)} \\ \mathbf{0} & 0 & 1 & \cdots & 0 \\ \vdots & \vdots & \vdots & \vdots & \vdots \\ \mathbf{0} & 0 & 0 & \cdots & 1 \\ \mathbf{0} & 0 & 0 & \cdots & 0 \end{pmatrix}_{(2m-1)\times(2m-1)} \quad \text{and} \quad \tilde{\mathbf{B}} = \begin{pmatrix} \mathbf{B}^{(1)} \\ 0 \\ \vdots \\ 0 \\ 1 \end{pmatrix}_{(2m-1)\times 1}. \quad (3)$$

$\mathbf{0}$ indicates an m-dimensional row vector of 0's. Note that eigenvalues of $\mathbf{A}$ are eigenvalues of $\tilde{\mathbf{A}}$ with corresponding eigenvectors $\mathbf{k}_i = (\mathbf{e}_i^T, 0, \ldots, 0, 0)^T$, $i = 1, 2, \ldots, m$. Clearly these m vectors are not enough to span the $(2m-1)$-dimensional expanded phase space. As in Ref. [13], additional vectors can be found in the null space of the matrix $\tilde{\mathbf{A}}^{m-1}$.

To determine the target point, let ε be the noise level in the system. A target point is chosen as $\delta\mathbf{Y}_T \equiv \mathbf{Y}_T - \mathbf{Y}^* = \tilde{\mathbf{A}}\varepsilon\sum_{i=1}^{u}\mathbf{k}_i$, which is one iterate away from the noise circle along the unstable directions. Here we make the assumption that the target is not too far away from the periodic saddle so that the same linearized dynamics applies near the target point. Subtracting this from the expression describing the linear dynamics in the expanded phase space, we obtain

$$\mathbf{Y}_{n+1} - \mathbf{Y}_T = \tilde{\mathbf{A}}(\mathbf{Y}_n - \mathbf{Y}^*) + \tilde{\mathbf{B}}(p_n - p^*) - \tilde{\mathbf{A}}\varepsilon\sum_{i=1}^{u}\mathbf{k}_i.$$

We wait until the system trajectory reaches the neighborhood of $\mathbf{Y}^*$ and apply u small parametric perturbations $\delta p_n, \delta p_{n+1}, \delta p_{n+2}, \ldots, \delta p_{n+(u-1)}$ so that the subsequent deviation $\delta\mathbf{Y}'_{n+u} = \mathbf{Y}_{n+u} - \mathbf{Y}_T$ lies entirely in the stable subspace of the target point, which has the same properties as that of the saddle point in the linear approximation. We then set the parameter to its nominal value p^* and the orbit marches toward the chaotic saddle under the system's natural dynamics. Thus we determine the perturbation δp_n needed at time n to be

$$\delta p_n = -\sum_{k=1}^{u}\frac{(\lambda_k)^u\mathbf{v}_k^T\cdot\delta\mathbf{Y}_n - \lambda_k\varepsilon\mathbf{v}_k^{\mathrm{T}}\cdot\mathbf{k}_k}{(\mathbf{v}_k^{\mathrm{T}}\cdot\tilde{\mathbf{B}})\prod_{\substack{i=1\\ i\neq k}}^{u}(\lambda_k - \lambda_i)}, \quad (4)$$

where the unstable contravariant eigenvector $\mathbf{v}_k$ is defined by $\tilde{\mathbf{A}}^{\mathrm{T}}\mathbf{v}_k = \lambda_k\mathbf{v}_k$. The first term is identical to the control law derived in Ref. [13], whereas the second term reflects the targeting of the point that is one mapping away from the noise circle along the unstable directions. Although future perturbations $\delta p_{n+1}, \ldots, \delta p_{n+(u-1)}$ can also be

found at the same time as δp_n, system noise makes it preferable to recalculate the perturbation using Eq. (4) at each iterate n.

For simplicity, let $v_k^{(m)} = 1$. Then the other components of $\mathbf{v}_k$ are $v_k^{(i)} = \sum_{j=1}^{i} a^{(m-j+1)}/(\lambda_k)^{i-j+1}$, $i = 1, 2, \ldots, m-1$ and $v_k^{(i)} = \sum_{j=1}^{i-m} b^{(m-j+1)}/(\lambda_k)^{i-m-j+1}$, $i = m+1, m+2, \ldots, 2m-1$. With these relations we emphasize that Eq. (4) depends only on the experimentally determined $a^{(i)}$, $b^{(i)}$, and the unstable eigenvalues λ_i $(i = 1, 2, \ldots, u)$ of $\mathbf{A}$.

Example 1: The Ikeda map.—The method is first demonstrated on the Ikeda map $z_{n+1} = a + bz_n \times \exp[ik - i\eta/(1 + |z_n|^2)]$, where $z = x + iy$ is complex making the map 2D. For $a = 1.0027$, $b = 0.9$, $k = 0.4$, and $\eta = 6.0$, the map exhibits a boundary crisis [15] with the boundary saddle at $z = z^* = 1.112\,451 - i2.283\,082$. (Cf. Fig. 1.) a is the control parameter. Being an actual map, there is no dependence on the past history of the perturbations during control. Therefore the perturbations are described by $\delta p_n = -\lambda_u(f_u^{(1)}\delta x + f_u^{(2)}\delta y - \varepsilon)/(f_u^{(1)}b_1^{(1)} + f_u^{(2)}b_2^{(1)})$. λ_u is the unstable eigenvalue of the 2×2 Jacobian matrix $\mathbf{A}$ evaluated at the saddle point. ε is chosen to be 0.005 so that the target point can be distinguished in Fig. 1, although a much smaller value for ε can be used. To determine $b_1^{(1)}$ and $b_2^{(1)}$, a perturbation $\delta p_n = 0.1000$ was applied when a point entered the linear region of radius 0.035 829 of the saddle. $b_1^{(1)}$ and $b_2^{(1)}$ were 1.00 156 and 0.001 134, respectively.

Figure 1(a) shows the orbit as it traverses the remnant chaotic attractor. After a time, the orbit approaches the boundary saddle along the right side of its stable manifold and that path carries it out toward a distant attractor. Figure 1(b) expands the square in Fig. 1(a). Points $1'-5'$ mark the escape toward the distant attractor. Restarting the simulation with the same initial conditions, we apply the maintenance technique. When the orbit starts to approach the boundary saddle, a perturbation is given to prevent point 2 from mapping to point $3'$, causing it instead to map to point 3. Note that only a single perturbation was given because the stable point has only one unstable direction and noise was not a consideration. After this the parameter is set to its nominal value and the natural dynamics of the saddle carries the orbit back onto the chaotic remnant (points 4–8).

Example 2: The magnetoelastic ribbon experiment.—The experimental system is a gravitationally buckled, amorphous magnetoelastic ribbon whose Young's modulus can be varied by a factor of 10 using an external magnetic field. (For details, see Ref. [16].) The ribbon is clamped at its base and a fotonic sensor mounted a short distance above the base measures its position. A vertical field $H_{\text{applied}}(t) = H_{\text{dc}} + H_{\text{ac}}\sin(2\pi ft)$ is applied to vary the ribbon's stiffness. H_{ac} is the control parameter as well as the bifurcation parameter. We set $f = 0.90$ Hz, $H_{\text{dc}} = 0.2980$ Oe, and $H_{\text{ac}} = 1.1124$ Oe to put the system slightly past the critical parameter $H_{\text{ac}}^{\text{critical}} \cong 1.1036$ Oe for a boundary crisis.

False nearest-neighbor tests show that the embedding dimension for this experiment is $m = 3$. The boundary saddle was determined to be an unstable period-1 orbit located at (2.6505, 2.6505, 2.6505). Nine close approaches to the boundary saddle were used to determine the elements of $\mathbf{A}$. Using singular value decomposition, $a^{(1)}$, $a^{(2)}$, and $a^{(3)}$ were 2.5016, 0.6727, and 0.1939, respectively. Thus, from $\mathbf{A}$, the saddle has one unstable and two complex stable eigenvalues, $\lambda_u = 2.7697$ and $\lambda_s^{1,2} = -0.1341 \mp i0.2281$, respectively.

The elements $b^{(1)}$, $b^{(2)}$, and $b^{(3)}$ were determined by applying a perturbation $\delta p_n = 0.0155$ Oe at a time n when the point closely approached the saddle. The perturbation

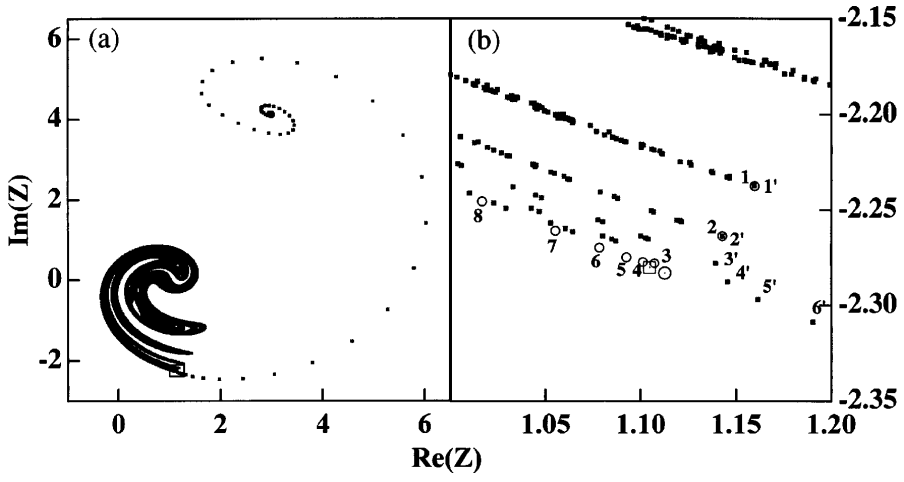

FIG. 1. (a) The Ikeda map at boundary crisis. The system resides on the chaotic transient (lower left) before exiting to the fixed point attractor (upper right). (b) Expands the square area in (a) to show details near the saddle point (large circle with centered dot). $1'-5'$ indicate the escape to the fixed point attractor. The circles (1–8) denote the perturbed orbits as they were diverted toward the chaos. The large square with centered dot is the target.

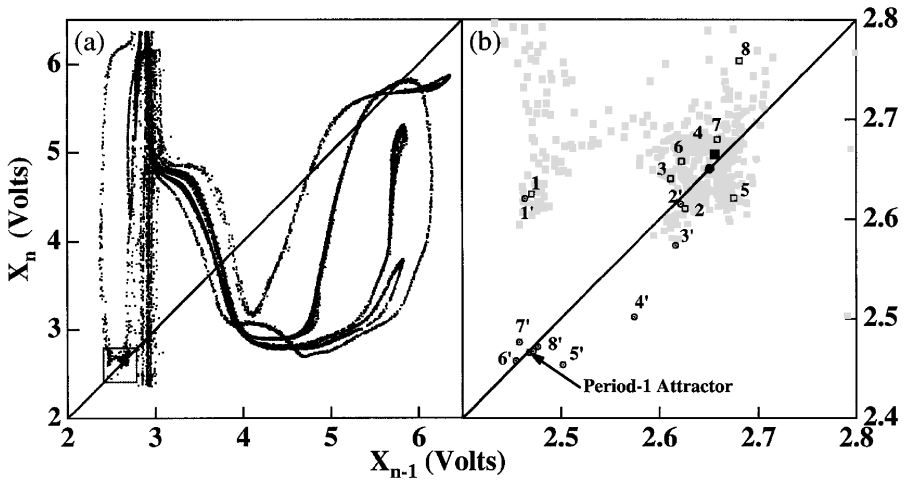

FIG. 2. (a) 2D projection of the transiently chaotic ribbon attractor. (b) Expands the square area in (a). Two nearby escape sequences are marked to illustrate the perturbed sequence (small squares 1–8) and the unperturbed one (small circles $1'-8'$). The filled circle on the diagonal marks the saddle point and the filled square marks the target. Perturbations were always given in the cluster around the saddle point.

lasts for the full duration of one drive (map) period. We use the measurements at times $n + 1$, $n + 2$, and $n + 3$ to calculate the $b^{(1)}$, $b^{(2)}$, and $b^{(3)}$ as $b^{(i)} = (\delta x_{n+i} - a^{(1)}\delta x_{n+i-1} - a^{(2)}\delta x_{n+i-2} - a^{(3)}\delta x_{n+i-3})/\delta p_n$. Typical values of $b^{(1)}$, $b^{(2)}$, and $b^{(3)}$ are 0.0024, 0.0046, and 0.0074 V/Oe, respectively. For typical runs in this experiment ε was 0.0100 V.

Using these values, we have maintained chaos in the ribbon experiment. Figure 2(a) plots in 2D the ribbon attractor for 51 712 iterates. For the first 51 123 iterates the ribbon made 51 approaches to the saddle and all were diverted toward the target and eventually made their way back to the chaotic attractor. After iterate 51 200, maintenance was turned off. At iterate 51 520 the system made a transition to the periodic attractor. Figure 2(b) expands a section of this attractor along with two nearby sequences. The unprimed sequence indicates the perturbed orbit. Starting at orbit 2, several successive perturbations were applied to push this sequence of orbits toward the target region. When the system approached the target *in* 3D, the perturbation was turned off to allow the natural dynamics to carry the system back into chaos. Primed points indicate the unperturbed orbit that made its way toward the period-1 attractor.

In conclusion, we have developed a general theory for the maintenance of chaos. This method uses small time-dependent perturbations of a single system parameter to perturb the system while it is in the vicinity of a mediating saddle point that possesses an arbitrary number of stable and unstable manifolds. The method was demonstrated computationally on the Ikeda map and experimentally on the magnetoelastic ribbon experiment. Even though the method was developed and tested for crisis bifurcations, it is well-suited for maintaining chaos against intermittencies as well.

V. I. gratefully acknowledges support from the ASEE/ONR Fellowship Program and M. L. S. acknowledges support from the NSWC ILIR Program and from the Office of Naval Research (Physical Sciences Division).

[1] J. M. Ottino, G. Metcalfe, and S. C. Jana, in *Proceedings of the 2nd Experimental Chaos Conference*, edited by W. Ditto *et al.* (World Scientific, Singapore, 1995), p. 3–20.
[2] A. L. Goldberger, in *Proceedings of the 1st Experimental Chaos Conference*, edited by S. Vohra *et al.* (World Scientific, Singapore, 1991), pp. 195–202.
[3] C. S. Daw, J. F. Thomas, G. A. Richards, and L. L. Narayanaswami, Chaos **5**, 662 (1995).
[4] V. In, M. L. Spano, J. D. Neff, W. L. Ditto, C. S. Daw, K. D. Edwards, and K. Nguyen, Chaos **7**, 605 (1997).
[5] S. J. Schiff, K. Jerger, D. H. Duong, T. Chang, M. L. Spano, and W. L. Ditto, Nature (London) **370**, 615 (1994).
[6] W. Yang, M. Ding, A. Mandell, and E. Ott, Phys. Rev. E **51**, 102 (1995).
[7] V. In, S. E. Mahan, W. L. Ditto, and M. L. Spano, Phys. Rev. Lett. **74**, 4420 (1995).
[8] G. Chen and D. Lai, Technology Report No. 95-90, 1995.
[9] I. B. Schwartz and I. Triandaf, Phys. Rev. Lett. **77**, 4740 (1996).
[10] E. Ott, *Chaos in Dynamical Systems* (Cambridge Univ. Press, New York, 1993), p. 277.
[11] F. Takens, *Dynamical Systems and Turbulence*, edited by D. Rand and L. S. Young (Springer-Verlag, Berlin, 1981), p. 230; N. H. Packard *et al.*, Phys. Rev. Lett. **45**, 712 (1980); J. P. Eckmann and D. Ruelle, Rev. Mod. Phys. **57**, 617 (1985).
[12] U. Dressler and G. Nitsche, Phys. Rev. Lett. **68**, 1 (1992).
[13] M. Ding, W. Yang, V. In, W. L. Ditto, M. L. Spano, and B. Gluckman, Phys. Rev. E **53**, 4334 (1996).
[14] P. So and E. Ott, Phys. Rev. E **51**, 2955 (1995).
[15] C. Grebogi, E. Ott, and J. A. Yorke, Phys. Rev. Lett. **57**, 1284 (1986).
[16] W. L. Ditto *et al.*, Phys. Rev. Lett. **63**, 923 (1989).